Global Satellite-Based Coastal Bathymetry from Waves

Rafael Almar [1,*], Erwin W. J. Bergsma [2], Gregoire Thoumyre [1], Mohamed Wassim Baba [1,3], Guillaume Cesbron [1,4], Christopher Daly [1], Thierry Garlan [5] and Anne Lifermann [2]

1   Laboratoire d'Etudes en Géophysique et Océanographie Spatiales (LEGOS),
    Université de Toulouse/CNRS/CNES/IRD, 31400 Toulouse, France;
    gregoire.thoumyre@legos.obs-mip.fr (G.T.); wassim.baba@um6p.ma (M.W.B.);
    guillaume.cesbron@legos.obs-mip.fr (G.C.); christopher.daly@legos.obs-mip.fr (C.D.)
2   French Space Agency (CNES), 75039 Paris, France; Erwin.Bergsma@cnes.fr (E.W.J.B.);
    Anne.Lifermann@cnes.fr (A.L.)
3   Center for Remote Sensing Application (CRSA), University Mohammed VI Polytechnic (UM6P),
    Benguerir 43150, Morocco
4   Mercator-Ocean International, 31400 Toulouse, France
5   Service Hydrographique et Océanographique de la Marine (SHOM), 29240 Brest, France;
    thierry.garlan@shom.fr
*   Correspondence: rafael.almar@ird.fr

Abstract: The seafloor—or bathymetry—of the world's coastal waters remains largely unknown despite its primary importance to human activities and ecosystems. Here we present S2Shores (Satellite to Shores), the first sub-kilometer global atlas of coastal bathymetry based on depth inversion from wave kinematics captured by the Sentinel-2 constellation. The methodology reveals coastal seafloors up to a hundred meters in depth which allows covering most continental shelves and represents 4.9 million km^2 along the world coastline. Although the vertical accuracy (RMSE 6–9 m) is currently coarser than that of traditional surveying techniques, S2Shores is of particular interest to countries that do not have the means to carry out in situ surveys and to unexplored regions such as polar areas. S2Shores is a major step forward in mitigating the effects of global changes on coastal communities and ecosystems by providing scientists, engineers, and policy makers with new science-based decision tools.

Keywords: coastal ocean; satellite earth observation; wave kinematics bathymetry; remote sensing; optical imagery

1. Introduction

The submerged surface of the coastline represents the invisible but largest fraction of the coastal zone. It is perhaps the most important part of the coastal system in terms of exposure of coastal populations and ecosystems to erosion and flooding [1], but despite its importance, coastal bathymetries and their influence are often overlooked. The main reason for this is the current lack of comprehensive information on coastal bathymetry, when the existing is often local and/or focused on economically interesting areas [2]. In addition, coastal maps and surveys are often decades old, largely out of date, or simply nonexistent in large parts of the world. This is particularly a problem for the 40% of the world's coastal sandy regions [3] that are the most dynamic geological environments on Earth. Overall, this missing bathymetry information limits our ability to understand and predict coastal evolution which on its own inherently leads to large uncertainties in predicting hazards such as coastal sea states, storm surges, and wave-induced surges and flooding [4–6]. The availability of fast, inexpensive, and efficient methods is also needed for studies of bottom variability, such as sandy shoreface or underwater dune dynamics but also some environmental applications such as benthic habitat mapping [7], seabed geomorphology [8], underwater archaeology [9], and exploration of unexploded

ordnance [10]. There is currently a growing demand for coastal monitoring, where coastal bathymetry is of critical importance [11,12].

On a global scale, hydrographic services cover less than 1% of their continental shelf each year, resulting in recurrent secular surveys. In addition, the shallow water reach of these campaigns is limited. Hence, depths ranging from 0 to 30 m have not been surveyed by sonar [13] and the use of expensive airborne LiDAR is required to cover this environment [14] and alternatively using UAV/drones locally [15,16]. These high-resolution surveys cover only a few percent of the world's coastlines, and the high variability of these environments poses the problem of the validity period of these surveys (IHO Survey Report C-55 [2,17]). Currently, international initiatives such as the GEBCO Seabed 2030 bathymetry mapping program [13] raises the need for coastal bathymetry solutions available on a global basis.

Satellite-derived bathymetry can provide a useful alternative. Thanks to the considerable advances in satellite coastal earth observation methods in recent years and increasing data availability [11,12], a number of academic and commercial satellite-derived bathymetry methodologies have emerged to exploit this potential [18]. This may be achieved using laser (LiDAR) [19–21], radar [22,23], and optical missions. For the latter, the two most advanced techniques which allow direct measurement of depth by satellite are water color [24–29] and wave kinematics [30–33]. Colour-based methods built from the pioneer work by [25] are limited to non-turbid waters. The wave kinematics methods work well in conditions where color-based methods would fail, namely in turbid or optically deep water, which is most of the open coastline worldwide where waves are experienced [34]. Wave characteristics change at varying depths, making depth accessible by remote sensing methods that aim to follow wave patterns [35]. Wave celerity and wavelength decrease as the waves sense the bottom and the depth decreases towards shore. The method then relies on how the satellite data can be used to capture wave patterns [36–38].

Here, we present S2Shores (Satellite to Shores), the first sub-kilometer global satellite-derived coastal bathymetry based on wave kinematics from the optical Sentinel-2 mission. We first present the methodology and computational approach, then show the prototype of global coastal bathymetry, which we compare to the local ground truth, and discuss the influence of environmental conditions and further developments towards an operational implementation.

2. Data and Methods

2.1. Wave-Based Bathymetry Inversion

The method employed in this work is amply documented [33,39–41]. As the water depth decreases toward the shore, the waves increasingly "feel" the bottom by increasing bottom friction until the waves eventually break near the shore. The dominance of wave propagation by depth can be described by a mathematical relationship: the dispersion relationship for free surface waves.

$$c^2 = \frac{g}{k} \tanh(kh) \Leftrightarrow h = \frac{\tanh^{-1}\left(\frac{c^2 k}{g}\right)}{k} \tag{1}$$

where c is wave phase celerity, k the wavenumber, and h the water depth and g is the gravitational acceleration (9.8 m/s^2 here). To solve Equation (1), we look for the pair of c and k. Here the wave phase shift (leading to celerity c) per k is computed from different detector bands using a discrete Fourier slicing technique based on a polar Radon transform [33,40,42]. The intensity signal $I(x, y)$ is first transformed into polar space $R_I(\theta, \rho)$ with the Radon transform (Equation (2)):

$$R_I(\theta, \rho) = {}_D I(x, y) \, \delta(\rho - x \cos(\theta) - y \sin(\theta)) \, dy \, dx \tag{2}$$

where $I(x, y)$ is the sub-sampled image, δ a Dirac function, ρ the beam length, and θ the rotational angle. A discrete Fourier transform can then be applied using Equation (3):

$$\tilde{H}(k) = \sum_{n=0}^{N-1} h_n(\rho) e^{-2\pi i k n / N} \tag{3}$$

wherein $\tilde{H}(k)$ is the discrete Fourier approximation of a continuous Fourier transform, $h_n(\rho)$ is the input signal per given angle—here obtained from the Radon sinogram over beam length ρ—k represents the angular wavenumber (frequency in space), n the current sample, and N is the total number of samples. Here we limit the angular wavenumbers associated with offshore wave periods (T) ranging from 3 to 25 s with a ΔT of 0.05 s.

The great advantage of this combination of discrete Fourier and Radon transform technique is the limited dependence on the computation window and image resolution to estimate the wave propagation while maintaining the computational performance [40].

The maximum depth (or deep water limit of the linear wave dispersion theory—Equation (1)) felt by the waves is between L/5 and L/3 [43] and is the theoretical range of application of the method (~20 to 200 m [40]).

2.2. Satellite Data Collection

S2Shores can run on any sensor capturing wave propagation [32,33]. We use here the Sentinel-2 constellation of the European Space Agency's COPERNICUS Earth observation program. The Sentinel-2 constellation started with the Sentinel-2A mission in 2015 and complemented in 2017 by Sentinel-2B, increasing the revisit from 10 to a few days depending on the latitude [34]. Sentinel-2 has 12 spectral bands with different resolutions, 10 m, 20 m, and 60 m. We use here the two 10 m bands B2 (blue, 490 nm) and B4 (red, 665 nm) because of their large relative time difference (dt = 1.005 s, see ESA S2 manual [44]) and a similar wave signature [33].

Sentinel 2 collects data up to 20 km off the coast (mission requirements in ESA Handbook [45]). The list of coastal tiles is obtained by setting the potential depth to 100 m to most continental shelves and islands using the General Bathymetric Chart of the Oceans (GEBCO [46], with horizontal resolution of 1/4 arc min, ~465 m), one of the few publicly available global bathymetric datasets along with ETOPO [47] of the National Oceanic and Atmospheric Administration (NOAA, with horizontal resolution of 1 arc min, ~1.85 km) [18].

2.3. Global Composite Bathymetry Computation

The full Sentinel 2 tiles, covering 100 km × 100 km, are divided into computational sub-tiles where wave celerity and wavelength are computed using a directional spectral method [33,40]. The bathymetry is then inverted using the linear wave dispersion relation (Equation (1)). While the computation window is in this case 800 m to cover multiple wavelengths, the output spatial horizontal resolution grid is here set to 500 m to match the GEBCO resolution. This implies here an overlap that acts as a moving average. At the local to regional scale (~10^4–10^6 km^2), the resolution can be increased down to a 100 m grid with no computational or physical limitation [33,41,48]. Such high resolution product potentially allows visualization of fine bottom features such as nearshore sandbars. Nonetheless, to compute the global coastal bathymetry at this high resolution would require significantly higher computational cost [39], and would therefore be more suitable for generating datasets on a local to regional level, using a higher-resolution satellite (i.e., 2 m of VENUS [40], 0.5 m of Pleiades, and 0.25 m of Pleiades Neo [32]). Overall, the orbit and swath settings of Sentinel-2 lead to more than 300 passes over the period 2015–2021 at a single location. From these data, the best satellite passes to estimate the bathymetry are selected using the ERA5 hindcast (from the European Centre for Medium-Range Weather Forecasts) that is hourly at a quarter degree resolution [49,50]. The optimal local conditions are defined as the greatest wave power ($\alpha H_s^2 T_p$, with H_s being the significant wave height and T_p being the peak period) and minimal clouds. From there, the top 10 passes for each Sentinel 2 tile are retained to generate the global S2Shores composite. The composite is made by assembling the bathymetry according to the preferred individual wave conditions: long waves are given more weight in deep water and short waves in shallow areas [40,51].

This is done using $\gamma = \frac{c^2 k}{g}$ [52,53] which tends to 1 at the deep-water limit, and 0 at the coastline. The individual resulting depths are combined and weighted using γ and the final result is a single depth to which several estimates contribute.

S2Shores has spatially varying depth application range worldwide with the shallowest extents at closed sea with short (<8 s) waves and deeper extents at open ocean coasts that experience long swells (~8 s–25 s) [34].

The estimated depths per Sentinel-2 image are referenced vertically to mean sea level. Per image, for each date and location, a corresponding tidal elevation is obtained using the FES2014 model [54] and this level is then subtracted from the obtained depth.

3. Results

3.1. The Global Coastal Bathymetry S2Shores

The S2Shores World product shown in Figure 1 uses up to 7000 tiles to cover the world's 1.5 million kilometers of coastline [55], continental lands, and islands. Wide and shallow shelves are well reached by our method, which goes deeper (up to hundreds of meters) on open coasts exposed to long swell waves in large basins (such as around the Pacific Ocean) and goes shallower (tens of meters) in closed seas (such as the Mediterranean and Red Sea, Persian Gulf) and wave-sheltered areas counting with short waves (such as the Indonesian archipelago and large estuaries such as Mar del Plata). Overall, waves are experienced at any coast [34] which allows a global application of S2Shores.
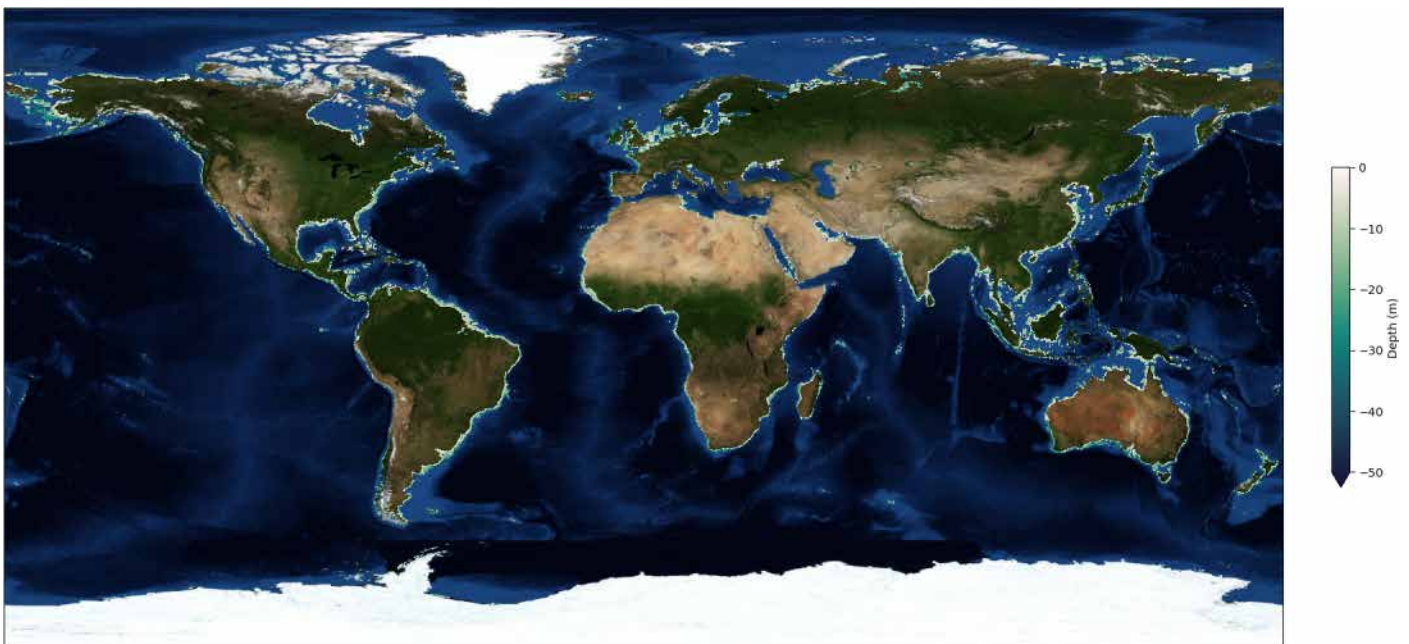

Figure 1. Global view of S2Shores satellite-derived bathymetry on MODIS true color image.

While a necessary coarse 500 m output grid resolution of the global S2Shores product cannot resolve very fine nearshore decimeter features such as sandbars, larger scale tidal channels and submarine dunes are revealed in deltas and at river mouths (e.g., Yangtze delta, China, in Figure 2, [56]). Offshore sediment banks, such as those found on muddy coasts (e.g., French Guyana, South America, Figure 2, [57]) are also captured by S2Shores, which is an important outcome for navigation safety. At different latitudes, the wide and relatively shallow shelves of Alaska, Senegal and East Coast of North America offer optimal conditions for S2Shores, but also the narrow and steep rugged coasts of Morocco and South Africa where S2Shores reaches deep waters. In Figure 2, the regions with fetch-limited or partially sheltered from waves at the Mediterranean Libyan gulf, Mar del Plata, and Portugal Tagus estuary illustrate that waves are experienced anywhere in the world over

a long enough period, despite a depth application range of S2Shores being reduced by short waves.
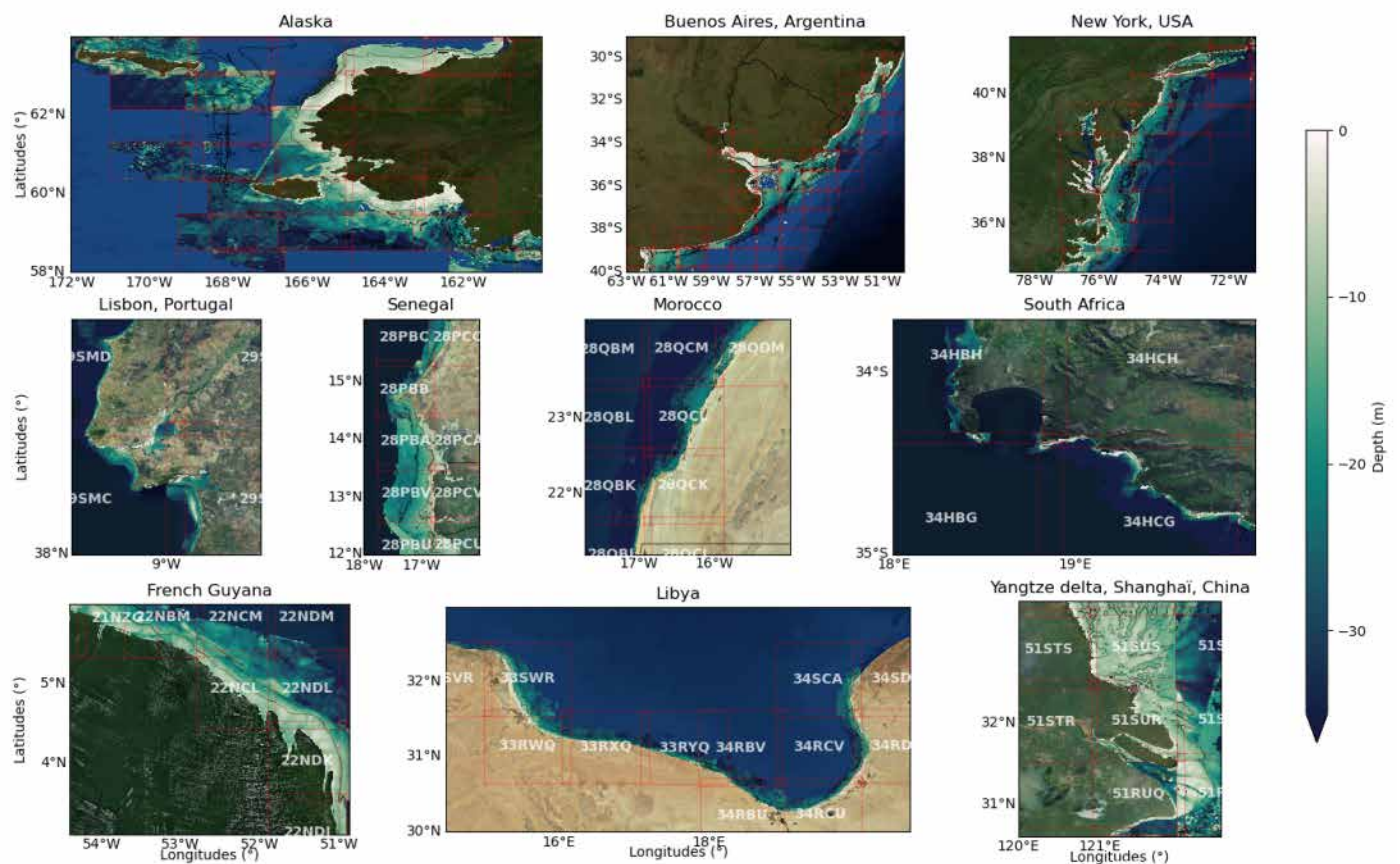

Figure 2. Illustration of S2Shores satellite-derived coastal bathymetry at hotspots worldwide on MODIS true color image. Red squares stand for Sentinel-2 tiles used.

3.2. Local Comparison with Ground Truth

A detailed comparison of S2Shores with the multibeam echosounder survey of the French Hydrographic and Oceanographic Office (SHOM) is performed at four contrasting sites (Figure 3); (1) mid-latitude closed and fetch-limited Mediterranean Sea (southeastern France), (2) the muddy coasts with very turbid waters (French Guiana, South America), (3) a rugged tropical Caribbean island (Guadeloupe) with multiple bed types (corals, beaches, etc.) and wave expositions, (4) and western Europe exposed to long North Atlantic swells (southwestern France). The acquisition dates of the composites and surveys do not necessary match, which can be a problem for very dynamic environments in shallow areas, muddy coasts, and estuaries. RMSE between 6 and 9 m are found with median errors between 3 and 6 m.These errors are still too large for operational use as they do not meet International Hydrographic Organization (IHO) standards and clearly cannot compete with surveys [18]. Nevertheless, they are rather consistent and provide an unprecedented global coastal bathymetry, in areas that were simply not covered by observations until now, where a first estimate is simply better than nothing [17].
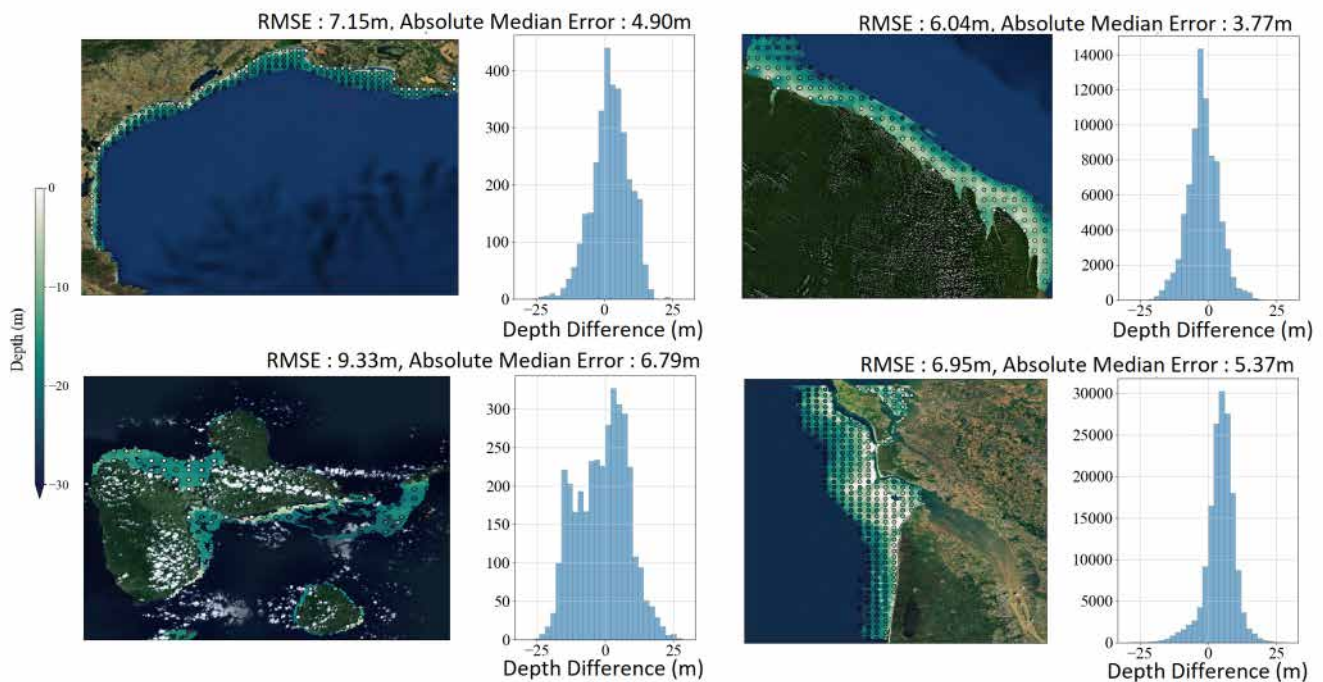
Figure 3. Comparison between S2Shores global satellite-based bathymetry with Naval Oceanographic and Hydrological Service (SHOM) multibeam sounder baseline surveys. The maps on the left show the S2Shores estimate with the surveys as colored circles and the error distribution on the right. (**top left**) French Mediterranean coast with fetch-limited waves, (**top right**) Guyane mud coast in South America, (**bottom left**) Guadeloupe island in the Caribbean and (**bottom right**) Gironde estuary in southwest France along the Atlantic Coast.

3.3. Global Error Analysis and Influence of Environmental Conditions

At the global scale, a cross-comparison is conducted with heterogeneous global product GEBCO, correlating on whole Sentinel-2 tiles the two products (Figure 4). The comparison shows good overall agreement, but also local discrepancies, sometimes between neighboring tiles. The latter can be explained by the fact that the 10-date composites are not necessarily from the same satellite passes. The 10-best passes are chosen based on the occurrence of locally maximum wave energy and lowest cloud coverage. Figure 4 also shows that there are no regional patterns. The correlation is generally not greater on open coasts in large-scale basins, confirming that waves are present all around the world's coasts [34] and can be captured by Sentinel-2 over a sufficiently long period (2015–2020 here). There is no latitude dependence. Clouds such as at the Equator and under mid-latitude storm tracks are thus not a problem when picking the clear sky passes. The polar regions show substantial correlations, indicating the potential of S2Shores in these remote regions. On a global scale, a multiple linear regression well predicts (r = 0.45) S2Shores scores in Figure 4 from local environmental conditions. The variables considered here by order of importance are: wave height, relative wave direction to the orbit, wave period, cloud cover, sun zenith angle, tidal level, and sun azimuth (Figure 5a). Figure 5b–g shows the global maps of average conditions encountered for all images at each tile. The waves experienced on open ocean coasts are larger and longer, which improves method accuracy. Wave crests in the direction of the orbit have low optical signature [58] and degrade accuracy. Moderate to high cloud cover is still present around the islands and high latitudes where the ERA5 cloud model could fail or where cloudy conditions are persistent with few moments of clear sky. Interestingly, tide, which is here corrected in term of bathymetry, has a degrading influence on wave propagation at shallow waters due to friction and currents. Research is underway to reduce the sensitivity of the method's performance to environmental conditions and to determine how the method can be adapted to a wider range of conditions encountered around the world.
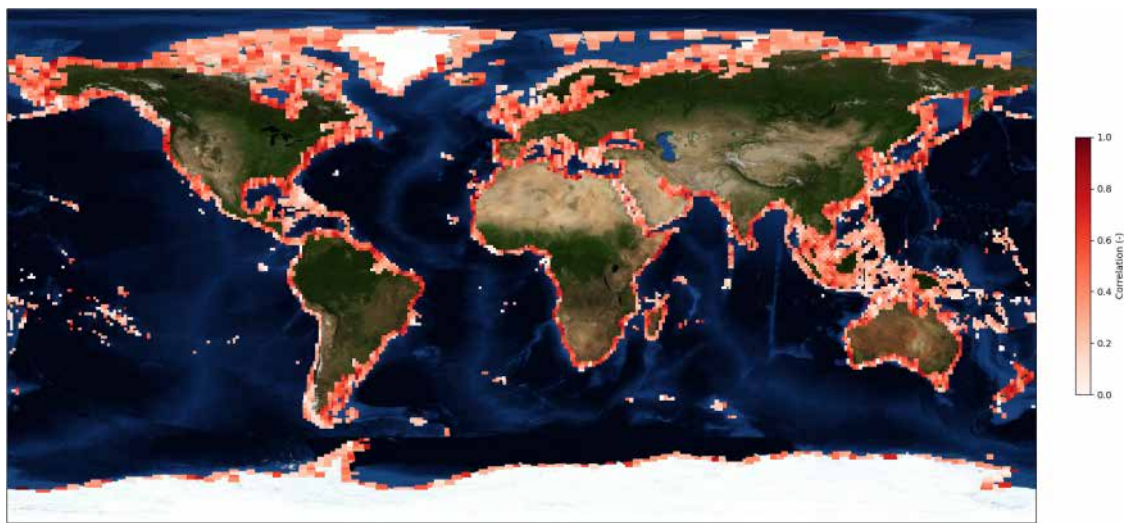
Figure 4. Correlation by tile between S2Shores satellite-derived bathymetry and GEBCO on MODIS true color image. While the Pearson correlation ranges between −1 and 1, the few negative correlations are shown as zero. The constant size of Sentinel-2 tiles in kilometers increases with latitude in this constant angle Mercator projection.
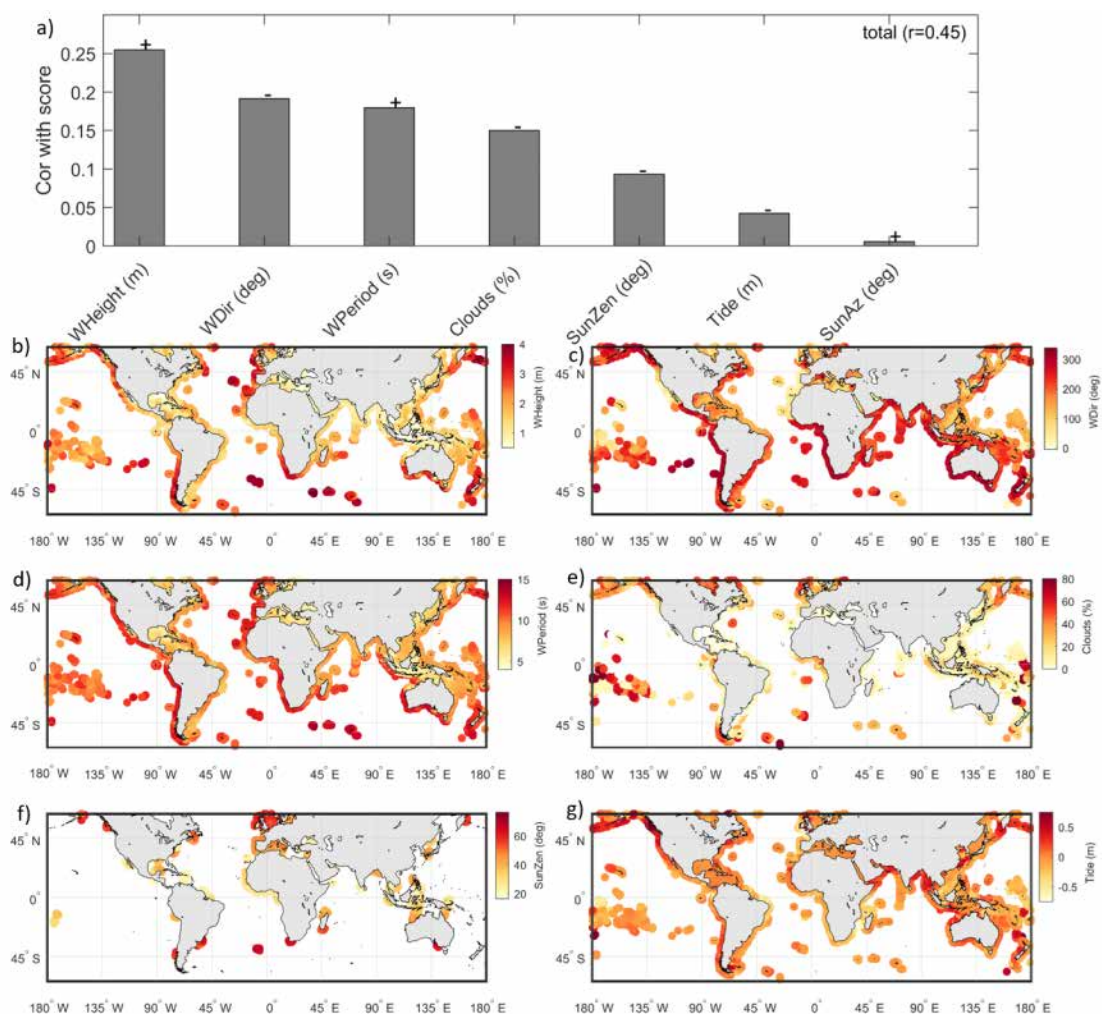

Figure 5. Influence of environmental conditions on S2Shores. (**a**) Global correlation of the method's score (correlation with GEBCO in Figure 4) with wave height (WHeight), relative wave direction to the orbit (WDir), wave period (WPeriod), cloud cover (Clouds), sun zenith angle (SunZen), tidal level (Tide), and sun azimuth (SunAz). Signs on top of bars indicate the type of positive or negative influence on method skills. (**b**–**g**) Global maps of average conditions experienced for all images at each tile.

4. Discussion

S2Shores performances are optimal at open coasts exposed to waves, and would fail in environments where LIDAR and color-based methods work well; namely in archipelagos, behind reef crests, in narrow bays, fjords, and other closed environments sheltered from waves. The finer resolution of LIDAR and color-based methods would allow sharp changes in depth to be better resolved, especially since wave-based methods are inherently physically limited by the wavelength and the time for waves to respond to a varying bottom.

A way to improve satellite-derived bathymetry accuracy is to combine different methods [18]. This can be achieved using laser (LiDAR) [19–21], radar [22,23], and optical satellite missions [58]. For non-wavy or clear waters, including a number of small islands, closed seas, and rugged coastlines—often sheltered from waves, lidar- and color-based methods offer an incomparable horizontal resolution and accuracy in the shallowest waters. Unlike these methods relying on water transparency, the wave-based approach enables depth estimation in coastal turbid areas and relatively deep water with a first pass estimated +58% (3.1 million km^2 when considering a very rough 14 m as a global average depth limit for visible bottoms for the color-based method [59–61]) potential gain in application coverage worldwide (Figure 6). Taking benefit of the rapid revisit of modern missions, good accuracy can be achieved for the foreshore at meso- to macrotidal environments with methods based on the detection of the shoreline at different tidal levels [62,63]. The benefits, drawbacks and limitations of these diverse methods suggest that these approaches are complementary and should be used in combination to cover coastal environments in their diversity.
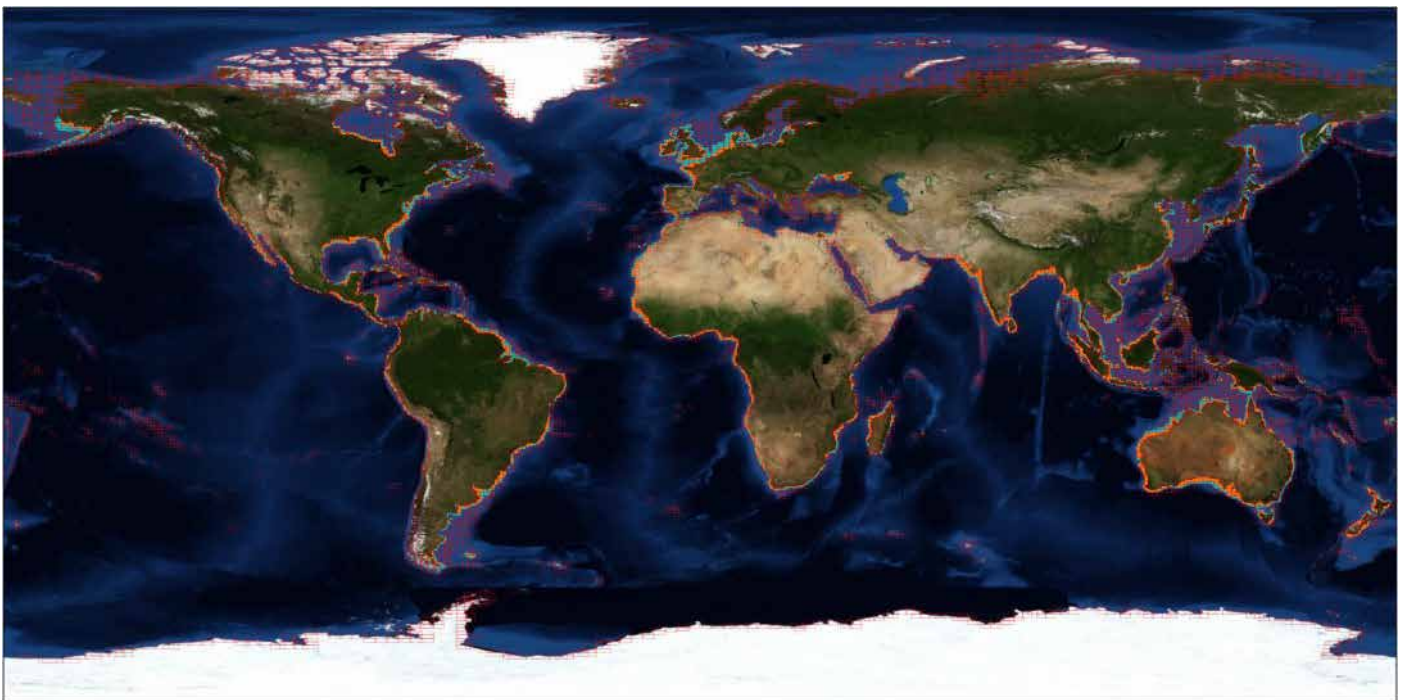

Figure 6. Global view of Sentinel-2 tiles (red squares) used for the present S2Shores Coastal bathymetry superimposed on MODIS true color image. Orange and blue areas are the regions covered by S2Shores with 50% and 2% wave occurrence conditions, respectively. Depths are extracted from GEBCO and waves from ERA5.

The ability to frequently and accurately monitor large-scale bathymetric changes will contribute significantly to expanding our understanding of dynamic coastal processes and their coupling to local human and large-scale climate forcing conditions. We currently have used images taken over a 5-year period using what can be considered as optimal conditions, with maximum wave energy and clear sky. S2Shores composites can be computed over shorter periods will offer the possibility to create unique time series of bathymetry and

thus observe dynamic changes in shallow water features, such as delta formations or underwater dune migration. The deepest regions are the less often monitored (2% regions in Figure 6, with 29 m global average maximum depth), while the shallowest regions have the potential for frequent monitoring (1.8 million km^2 with 17 m global average maximum depth). In particular, while Figure 4 indicates a global coverage, Figures 1 and 6 show that due to steep shoreface, there is only a narrow offshore number of potential applications at several places such as around the poles, West of South America and the Mediterranean Sea. In order to increase the signal-to-noise ratio, it is possible to produce composites of seasonal (3–4 months) to monthly changes in bathymetry on a regional scale. However, accurate detection of depths less than 20 m will be highly dependent on the probability of occurrence of successive high-energy wave conditions over a short time period. Thus, detection of bathymetric changes with reasonable accuracy over short periods of time will most likely be limited to shallow waters.

Significant efforts have recently been devoted to the development of operational numerical models at local and regional scales (e.g., early warning systems) to predict the impact of storms [5] and its link to socioeconomic and environmental risks [4,64,65]. However, the performance of these operational models is dampened by the lack of continuity between detailed local observations and necessarily coarse regional observations. Discontinuous spatio-temporal scales in observational and modeling strategies prevent an effective regional or global scale approach. For example, wave modeling in shallow waters is limited by the lack of bathymetry data and as a result a significant bias is introduced for extreme coastal water levels [66,67]. The few publicly available datasets with global coverage, mentioned above such as ETOPO (NOAA) and GEBCO, are created by using the gravity anomaly in satellite altimeter data, which relates to depth variations, to interpolate depths between in situ soundings [68,69]. Although these products are sufficient for deep water, they are not accurate in shallow or coastal areas [70,71]. Heterogeneous datasets lead to exaggerated artifacts at the coast, preventing their use for fine studies such as wave modeling for flooding purpose [72,73]. Several integration initiatives such as the EMODnet effort for Europe [18] aim to overcome this issue by correcting before accurately integrating bathymetric data from multiple sources such as the high-resolution multibeam echosounder and LiDAR bathymetry datasets available for Ireland as part of the Integrated Mapping for the Sustainable Development of Ireland's Marine Resource (INFOMAR) program [74]. Here, especially with its spatial coverage, S2Shores addresses this need, aiming to fill this existing observational scale gap with satellite, even with lower accuracy in comparison to local multibeam surveys [17]. The approach developed in S2Shores has, to our knowledge, no competing identified academic research project on a global basis, although private and public projects are starting to evolve in this direction [18]. S2Shores certainly strengthens the international effort (e.g., the collaborative project between GEBCO and the Nippon Foundation with the aim of facilitating the complete mapping of the global ocean floor by the year 2030—[13]) and research capacity by providing a baseline dataset and a renewed vision of our coasts.

5. Conclusions

Here we show that the combination of high-resolution satellite earth observation missions such as the Sentinel-2 (ESA) COPERNICUS optical constellation and the latest wave-based bathymetry inversion methodology can be used to derive global coastal bathymetry. The global S2Shores 500 m gridded product reveals the coastal bathymetry of 4.9 million km^2 with more than half of unexplored areas or decade-old coastal charts. The depth application range varies locally from a few meters on closed coasts exposed to short wind waves to a hundred of meters on open coasts exposed to long swells. A global analysis of the sensitivity of the method to environmental conditions shows that the method performs better with clear skies and low-angled sun, long and large waves coming with a cross-track crests direction. Although less accurate than conventional in situ surveys with a RMSE between 6 and 9 m when compared locally with ground truth, S2Shores is

the first global pass estimate available to date. Undoubtedly, these types of methodologies will be refined to gain accuracy and combined with other sensors and methods, opening the possibility of capturing morphological evolution. The future of satellite-derived bathymetry is bright, as the roadmap for future missions shows increasing data availability, resolution, and revisit, which will meet the growing demand for coastal bathymetry for coastal engineering, management and planning, forecasting, and coastal hazard mitigation.

References

1. Anthony, E.J.; Aagaard, T. The lower shoreface: Morphodynamics and sediment connectivity with the upper shoreface and beach. *Earth-Sci. Rev.* **2020**, *210*, 103334. [CrossRef]
2. Wölfl, A.C.; Snaith, H.; Amirebrahimi, S.; Devey, C.W.; Dorschel, B.; Ferrini, V.; Huvenne, V.A.I.; Jakobsson, M.; Jencks, J.; Johnston, G.; et al. Seafloor Mapping—The Challenge of a Truly Global Ocean Bathymetry. *Front. Mar. Sci.* **2019**, *6*, 283. [CrossRef]
3. Luijendijk, A. The State of the World's Beaches. *Sci. Rep.* **2018**, *8*, 6641. [CrossRef] [PubMed]
4. Vousdoukas, M.I.; Mentaschi, L.; Voukouvalas, E.; Bianchi, A.; Dottori, F.; Feyen, L. Climatic and socioeconomic controls of future coastal flood risk in Europe. *Nat. Clim. Chang.* **2018**, *8*, 776–780. [CrossRef]
5. Mentaschi, L.; Vousdoukas, M.; Pekel, J.F.; Voukouvalas, E.; Feyen, L. Global long-term observations of coastal erosion and accretion. *Sci. Rep.* **2018**, *8*, 12876. [CrossRef] [PubMed]
6. Almar, R.; Ranasinghe, R.; Bergsma, E.; Diaz, H.; Melet, A.; Papa, F.; Vousdoukas, M.; Athanasiou, P.; Dada, O.; Almeida, L.P.; et al. How waves are accelerating global coastal overtopping. *Nat. Commun.* **2021**, *12*, 3775. [CrossRef]
7. Janowski, L.; Wroblewski, R.; Dworniczak, J.; Kolakowski, M.; Rogowska, K.; Wojcik, M.; Gajewski, J. Offshore benthic habitat mapping based on object-based image analysis and geomorphometric approach. A case study from the Slupsk Bank, Southern Baltic Sea. *Sci. Total Environ.* **2021**, *801*, 149712. [CrossRef] [PubMed]
8. Summers, G.; Lim, A.; Wheeler, A.J. A Scalable, Supervised Classification of Seabed Sediment Waves Using an Object-Based Image Analysis Approach. *Remote Sens.* **2021**, *13*, 2317. [CrossRef]
9. Madricardo, F.; Bassani, M.; D'Acunto, G.; Calandriello, A.; Foglini, F. New evidence of a Roman road in the Venice Lagoon (Italy) based on high resolution seafloor reconstruction. *Sci. Rep.* **2021**, *11*, 13985. [CrossRef] [PubMed]
10. Czub, M.; Kotwicki, L.; Lang, T.; Sanderson, H.; Klusek, Z.; Grabowski, M.; Szubska, M.; Jakacki, J.; Andrzejewski, J.; Rak, D.; et al. Deep sea habitats in the chemical warfare dumping areas of the Baltic Sea. *Sci. Total Environ.* **2018**, *616–617*, 1485–1497. [CrossRef]
11. Benveniste, J.; Cazenave, A.; Vignudelli, S.; Fenoglio-Marc, L.; Shah, R.; Almar, R.; Andersen, O.; Birol, F.; Bonnefond, P.; Bouffard, J.; et al. Requirements for a Coastal Hazards Observing System. *Front. Mar. Sci.* **2019**, *6*, 348. [CrossRef]
12. Melet, A.; Teatini, P.; Le Cozannet, G.; Jamet, C.; Conversi, A.; Benveniste, J.; Almar, R. Earth observations for monitoring marine coastal hazards and their drivers. *Surv. Geophys.* **2020**, in press. [CrossRef]
13. Mayer, L.; Jakobsson, M.; Allen, G.; Dorschel, B.; Falconer, R.; Ferrini, V.; Lamarche, G.; Snaith, H.; Weatherall, P. The nippon foundation—GEBCO seabed 2030 project: The quest to see the world's oceans completely mapped by 2030. *Geosciences* **2018**, *8*, 63. [CrossRef]
14. Saylam, K.; Hupp, J.R.; Averett, A.R.; Gutelius, W.F.; Gelhar, B.W. Airborne lidar bathymetry: Assessing quality assurance and quality control methods with Leica Chiroptera examples. *Int. J. Remote Sens.* **2018**, *39*, 2518–2542. [CrossRef]
15. Agrafiotis, P.; Skarlatos, D.; Georgopoulos, A.; Karantzalos, K. Shallow water bathymetry mapping from uav imagery based on machine learning. *Int. Arch. Photogramm. Remote Sens. Spat. Inf. Sci.* **2019**, *XLII-2/W10*, 9–16. [CrossRef]

16. Bergsma, E.W.J.; Almar, R.; de Almeida, L.P.M.; Sall, M. On the operational use of UAVs for video-derived bathymetry. *Coast. Eng.* **2019**, *152*, 103527. [CrossRef]

17. Laporte, J.; Dolou, H.; Avis, J.; Arino, O. Thirty years of Satellite Derived Bathymetry: The charting tool that Hydrographers can no longer ignore. *Int. Hydrogr. Rev.* **2020**, *25*, 129–154.

18. Cesbron, G.; Melet, A.; Almar, R.; Lifermann, A.; Tullot, D.; Crosnier, L. Pan-European Satellite-Derived Coastal Bathymetry—Review, User Needs and Future Services. *Front. Mar. Sci.* **2021**. [CrossRef]

19. Abdallah, H.; Bailly, J.S.; Baghdadi, N.N.; Saint-Geours, N.N.; Fabre, F. Potential of Space-Borne LiDAR Sensors for Global Bathymetry in Coastal and Inland Waters. *IEEE J. Sel. Top. Appl. Earth Obs. Remote Sens.* **2013**, *6*, 202–216. [CrossRef]

20. Parrish, C.E.; Magruder, L.A.; Neuenschwander, A.L.; Forfinski-Sarkozi, N.; Alonzo, M.; Jasinski, M. Validation of ICESat-2 ATLAS Bathymetry and Analysis of ATLAS's Bathymetric Mapping Performance. *Remote Sens.* **2019**, *11*, 1634. [CrossRef]

21. Thomas, N.; Pertiwi, A.P.; Traganos, D.; Lagomasino, D.; Poursanidis, D.; Moreno, S.; Fatoyinbo, L. Space-Borne Cloud-Native Satellite-Derived Bathymetry (SDB) Models Using ICESat-2 And Sentinel-2. *Geophys. Res. Lett.* **2021**, *48*, e2020GL092170. [CrossRef]

22. Stewart, C.; Renga, D.A.; Gaffney, P.V.; Schiavon, P.G. Sentinel-1 bathymetry for North Sea palaeolandscape analysis. *Int. J. Remote Sens.* **2016**, *37*, 471–491. [CrossRef]

23. Bian, X.; Shao, Y.; Zhang, C.; Xie, C.; Tian, W. The feasibility of assessing swell-based bathymetry using SAR imagery from orbiting satellites. *ISPRS J. Photogramm. Remote Sens.* **2020**, *168*, 124–130. [CrossRef]

24. Stumpf, R.P.; Holderied, K.; Sinclair, M. Determination of water depth with high-resolution satellite imagery over variable bottom types. *Limnol. Oceanogr.* **2003**, *48*, 547–556. [CrossRef]

25. Lyzenga, D.R.; Malinas, N.P.; Tanis, F.J. Multispectral bathymetry using a simple physically based algorithm. *IEEE Trans. Geosci. Remote Sens.* **2006**, *44*, 2251–2259. [CrossRef]

26. Lee, Z.; Hu, C.; Casey, B.; Shang, S.; Dierssen, H.; Arnone, R. Global Shallow-Water From Satellite Ocean Color Data. *Eos* **2010**, *91*, 429–430. [CrossRef]

27. Hodúl, M.; Bird, S.; Knudby, A.; Chénier, R. Satellite derived photogrammetric bathymetry. *ISPRS J. Photogramm. Remote Sens.* **2018**, *142*, 268–277. [CrossRef]

28. Caballero, I.; Stumpf, R.P. Retrieval of nearshore bathymetry from Sentinel-2A and 2B satellites in South Florida coastal waters. *Estuarine Coast. Shelf Sci.* **2019**, *226*, 106277. [CrossRef]

29. Li, J.; Knapp, D.E.; Lyons, M.; Roelfsema, C.; Phinn, S.; Schill, S.R.; Asner, G.P. Automated Global Shallow Water Bathymetry Mapping Using Google Earth Engine. *Remote Sens.* **2021**, *13*, 1469. [CrossRef]

30. Poupardin, A.; Idier, D.; de Michele, M.; Raucoules, D. Water Depth Inversion From a Single SPOT-5 Dataset. *IEEE Transctions Geosci. Remote Sens.* **2016**, *54*, 2329–2342. [CrossRef]

31. Danilo, C.; Melgani, F. Wave Period and Coastal Bathymetry Using Wave Propagation on Optical Images. *IEEE Trans. Geosci. Remote Sens.* **2016**, *54*, 6307–6319. [CrossRef]

32. Almar, R.; Bergsma, E.W.J.; Maisongrande, P.; Almeida, L.P.M. Wave-derived coastal bathymetry from satellite video imagery: A showcase with Pleiades persistent mode. *Remote Sens. Environ.* **2019**, *231*, 111263. [CrossRef]

33. Bergsma, E.W.J.; Almar, R.; Maisongrande, P. Radon-Augmented Sentinel-2 Satellite Imagery to DeriveWave-Patterns and Regional Bathymetry. *Remote Sens.* **2019**, *11*, 1918. [CrossRef]

34. Bergsma, E.W.J.; Almar, R. Coastal coverage of ESA' Sentinel 2 mission. *Adv. Space Res.* **2020**, *65*, 2636–2644. [CrossRef]

35. Holman, R.A.; Plant, N.; Holland, T. cBathy: A Robust Algorithm For Estimating Nearshore Bathymetry. *J. Geophys. Res. Oceans* **2013**, *118*, 2595–2609. [CrossRef]

36. Kudryavtsev, V.; Yurovskaya, M.; Chapron, B.; Collard, F.; Donlon, C. Sun glitter imagery of ocean surface waves. Part 1: Directional spectrum retrieval and validation. *J. Geophys. Res.-Ocean.* **2017**, *122*, 1369–1383. [CrossRef]

37. Almar, R.; Bergsma, E.W.J.; Catalan, P.A.; Cienfuegos, R.; Suarez, L.; Lucero, F.; Nicolae Lerma, A.; Desmazes, F.; Perugini, E.; Palmsten, M.L.; et al. Sea State from Single Optical Images: A Methodology to Derive Wind-Generated Ocean Waves from Cameras, Drones and Satellites. *Remote Sens.* **2021**, *13*, 679. [CrossRef]

38. Ardhuin, F.; Stopa, J.E.; Chapron, B.; Collard, F.; Husson, R.; Jensen, R.E.; Johannessen, J.; Mouche, A.; Passaro, M.; Quartly, G.D.; et al. Observing Sea States. *Front. Mar. Sci.* **2019**, *6*, 124. [CrossRef]

39. Baba, W.M.; Bergsma, E.W.J.; Almar, R.; Daly, C.J. Deriving large-scale coastal bathymetry from Sentinel-2 images using an High-Performance Cluster: A case study covering North Africa's coastal zone. *Sensors* **2021**, *21*, 7006. [CrossRef]

40. Bergsma, E.W.J.; Almar, R.; Rolland, A.; Binet, R.; Brodie, K.L.; Bak, A.S. Coastal morphology from space: A showcase of monitoring the topography-bathymetry continuum. *Remote Sens. Environ.* **2021**, *261*, 112469. [CrossRef]

41. Daly, C.J.; Baba, W.; Bergsma, E.; Almar, R.; Garlan, T. The New Era of Regional Coastal Bathymetry from Space: A Showcase for West Africa using Sentinel-2 Imagery. *Remote Sens. Environ.* **2021**. [CrossRef]

42. Almar, R.; Michallet, H.; Cienfuegos, R.; Bonneton, P.; Tissier, M.; Ruessink, G. On the use of the Radon Transform in studying nearshore wave dynamics. *Coast. Eng.* **2014**, *92*, 24–30. [CrossRef]

43. Thuan, D.H.; Almar, R.; Marchesiello, P.; Viet, N.T. Video Sensing of Nearshore Bathymetry Evolution with Error Estimate. *J. Mar. Sci. Eng.* **2019**, *7*, 233. [CrossRef]

44. European Space Agency. ESA Sentinel 2 Orbit Description. 2019. Available online: https://sentinel.esa.int/web/sentinel/missions/sentinel-2/satellite-description/orbit (accessed on 9 January 2021).

45. European Space Agency. ESA Sentinel 2 Mission Scenario. 2019. Available online: https://sentinels.copernicus.eu/web/sentinel/missions/sentinel-2/observation-scenario (accessed on 9 January 2021).

46. GEBCO Compilation Group. GEBCO 2019 Grid. 2019. Available online: https://www.bodc.ac.uk/data/published_data_library/catalogue/10.5285/a29c5465-b138-234d-e053-6c86abc040b9/ (accessed on 29 November 2019).

47. National Geophysical Data Center, NESDIS, NOAA, U.S. Department of Commerce. *ETOPO1, Global 1 Arc-Minute Ocean Depth and Land Elevation from the US National Geophysical Data Center (NGDC)*; Department of Commerce, Research Data Archive at the National Center for Atmospheric Research, Computational and Information Systems Laboratory; National Geophysical Data Center, NESDIS, NOAA, U.S. Department of Commerce: Boulder, CO, USA, 2011. [CrossRef]

48. Almar, R.; Bergsma, E.W.J.; Gawehn, M.A.; Aarninkhof, S.G.J.; Benshila, R. High-frequency temporal wave-pattern reconstruction from a few satellite images: A new method towards estimating regional bathymetry. *J. Coast. Res.* **2020**, *95*, 996–1000. [CrossRef]

49. Dee, D.P.; Uppala, S.M.; Simmons, A.J.; Berrisford, P.; Poli, P.; Kobayashi, S.; Andrae, U.; Balmaseda, M.A.; Balsamo, G.; Bauer, P.; et al. The ERA-Interim reanalysis: Configuration and performance of the data assimilation system. *Q. J. R. Meteorol. Soc.* **2011**, *137*, 553–597. [CrossRef]

50. Copernicus Climate Change Service. ERA5: Fifth Generation of ECMWF Atmospheric Reanalyses of the Global Climate. 2017. Available online: https://cds.climate.copernicus.eu/cdsapp#!/home (accessed on 24 January 2021).

51. Bergsma, E.W.J.; Almar, R. Video-based depth inversion techniques, a method comparison with synthetic cases. *Coast. Eng.* **2018**, *138*, 199–209. [CrossRef]

52. Stockdon, H.F.; Holman, R.A. Estimation of wave phase speed and nearshore bathymetry from video imagery. *J. Geophys. Res.* **2000**, *105*, 22015–22033. [CrossRef]

53. Simarro, G.; Calvete, D.; Luque, P.; Orfila, A.; Ribas, F. UBathy: A New Approach for Bathymetric Inversion from Video Imagery. *Remote Sens.* **2019**, *11*, 2722. [CrossRef]

54. Carrere, L.; Lyard, F.H.; Cancet, M.; Guillot, A. Finite Element Solution FES2014, a new tidal model—Validation results and perspectives for improvements. In Proceedings of the ESA Living Planet Conference (2016), Prague, Czech Republic, 9–13 May 2016.

55. Burke, L. *Pilot Analysis of Global Ecosystems: Coastal Ecosystems*; World Resources Institute: Washington, DC, USA, 2001.

56. Guo, X.; Fan, D.; Zheng, S.; Wang, H.; Zhao, B.; Qin, C. Revisited sediment budget with latest bathymetric data in the highly altered Yangtze (Changjiang) Estuary. *Geomorphology* **2021**, *391*, 107873. [CrossRef]

57. Jolivet, M.; Anthony, E.J.; Gardel, A.; Brunier, G. Multi-Decadal to Short-Term Beach and Shoreline Mobility in a Complex River-Mouth Environment Affected by Mud From the Amazon. *Front. Earth Sci.* **2019**, *7*, 187. [CrossRef]

58. Ma, Y.; Xu, N.; Liu, Z.; Yang, B.; Yang, F.; Wang, X.H.; Li, S. Satellite-derived bathymetry using the ICESat-2 lidar and Sentinel-2 imagery datasets. *Remote Sens. Environ.* **2020**, *250*, 112047. [CrossRef]

59. Pacheco, A.; Horta, J.; Loureiro, C.; Ferreira, O. Retrieval of nearshore bathymetry from Landsat 8 images: A tool for coastal monitoring in shallow waters. *Remote Sens. Environ.* **2015**, *159*, 102–116. [CrossRef]

60. Chénier, R.; Faucher, M.A.; Ahola, R. Satellite-Derived Bathymetry for Improving Canadian Hydrographic Service Charts. *Int. J. Geo-Inf.* **2018**, *7*, 306. [CrossRef]

61. Traganos, D.; Poursanidis, D.; Aggarwal, B.; Chrysoulakis, N.; Reinartz, P. Estimating Satellite-Derived Bathymetry (SDB) with the Google Earth Engine and Sentinel-2. *Remote Sens.* **2018**, *10*, 859. [CrossRef]

62. Khan, M.J.U.; Ansary, M.N.; Durand, F.; Testut, L.; Ishaque, M.; Calmant, S.; Krien, Y.; Islam, A.S.; Papa, F. High-Resolution Intertidal Topography from Sentinel-2 Multi-Spectral Imagery: Synergy between Remote Sensing and Numerical Modeling. *Remote Sens.* **2019**, *11*, 2888. [CrossRef]

63. Fitton, J.M.; Rennie, A.F.; Hansom, J.D.; Muir, F.M. Remotely sensed mapping of the intertidal zone: A Sentinel-2 and Google Earth Engine methodology. *Remote Sens. Appl. Soc. Environ.* **2021**, *22*, 100499. [CrossRef]

64. Nicholls, R.J.; Hanson, S.E.; Lowe, J.A.; Warrick, R.A.; Lu, X.; Long, A.J. Sea-level scenarios for evaluating coastal impacts. *WIREs Clim. Chang.* **2014**, *5*, 129–150. [CrossRef]

65. Oppenheimer, M. Sea Level Rise and Implications for Low Lying Islands, Coasts and Communities. *IPCC Spec. Rep. Ocean Cryosph. Chang. Clim.* **2019**, *355*, 126–129.

66. Serafin, K.; Ruggiero, P.; Barnard, P.; Stockdon, H. The influence of shelf bathymetry and beach topography on extreme total water levels: Linking large-scale changes of the wave climate to local coastal hazards. *Coast. Eng.* **2019**, *150*, 1–17. [CrossRef]

67. Almar, R.; Marcos, M.; Le Cozannet, G.; Ranasinghe, R. Editorial: Coasts Under Changing Climate: Observations and Modeling. *Front. Mar. Sci.* **2021**, *8*, 1617. [CrossRef]

68. Smith, W.H.F.; Sandwell, D.T. Global Sea Floor Topography from Satellite Altimetry and Ship Depth Soundings. *Science* **1997**, *277*, 1956–1962. [CrossRef]

69. Smith, W.H.; Sandwell, D.T. Conventional Bathymetry, Bathymetry from Space, and Geodetic Altimetry. *Oceanography* **2004**, *17*, 8–23. [CrossRef]

70. Monteys, X.; Harris, P.; Caloca, S.; Cahalane, C. Spatial Prediction of Coastal Bathymetry Based on Multispectral Satellite Imagery and Multibeam Data. *Remote Sens.* **2015**, *7*, 13782–13806. [CrossRef]

71. Athanasiou, P.; van Dongeren, A.; Giardino, A.; Vousdoukas, M.; Gaytan-Aguilar, S.; Ranasinghe, R. Global distribution of nearshore slopes with implications for coastal retreat. *Earth Syst. Sci. Data* **2019**, *11*, 1515–1529. [CrossRef]

72. Melet, A.; Meyssignac, B.; Almar, R.; Le Cozannet, G. Under-estimated wave contribution to coastal sea-level rise. *Nat. Clim. Chang.* **2018**, *8*, 234–239 [CrossRef]
73. Kirezci, E.; Young, I.R.; Ranasinghe, R.; Muis, S.; Nicholls, R.J.; Lincke, D.; Hinkel, J. Projections of global-scale extreme sea levels and resulting episodic coastal flooding over the 21st Century. *Sci. Rep.* **2020**, *10*, 11629. [CrossRef] [PubMed]
74. Guinan, J.; McKeon, C.; O'Keeffe, E.; Monteys, X.; Sacchetti, F.; Coughlan, M.; Nic Aonghusa, C. INFOMAR data supports offshore energy development and marine spatial planning in the Irish offshore via the EMODnet Geology portal. *Q. J. Eng. Geol. Hydrogeol.* **2021**, *54*, qjegh2020-033. [CrossRef]